ESC European Society of Cardiology

European Heart Journal - Cardiovascular Imaging (2020) **21**, 93–101
doi:10.1093/ehjci/jez074

Magnetic resonance hyperpolarization imaging detects early myocardial dysfunction in a porcine model of right ventricular heart failure

Peter Agger[1]*, Janus Adler Hyldebrandt[2,3], Esben Søvsø Szocska Hansen[4], Camilla Omann[5], Nikolaj Bøgh[4], Farhad Waziri[5], Per Mose Nielsen[4], and Christoffer Laustsen[4]

[1]Comparative Medicine Lab, Department of Clinical Medicine, Aarhus University, Palle Juul-Jensens Boulevard 99, 8200 Aarhus, Denmark; [2]Department of Anaesthesiology and Intensive Care, Aarhus University Hospital, Palle Juul-Jensens Boulevard 99, 8200 Aarhus, Denmark; [3]Department of Anaesthesiology and Intensive Care, Akershus University Hospital, Sykehusveien 25, 1478 Lørenskog, Norway; [4]MR Research Centre, Aarhus University, Palle Juul-Jensens Boulevard 99, 8200 Aarhus, Denmark; and [5]Department of Cardiothoracic and Vascular Surgery, Aarhus University Hospital, Palle Juul-Jensens Boulevard 99, 8200 Aarhus, Denmark

Received 2 November 2018; editorial decision 26 March 2019; accepted 2 April 2019; online publish-ahead-of-print 27 April 2019

Aims Early detection of heart failure is important for timely treatment. During the development of heart failure, adaptive intracellular metabolic processes that evolve prior to macro-anatomic remodelling, could provide an early signal of impending failure. We hypothesized that metabolic imaging with hyperpolarized magnetic resonance would detect the early development of heart failure before conventional echocardiography could reveal cardiac dysfunction.

Methods and results Five 8.5 kg piglets were subjected to pulmonary banding and subsequently examined by [1-^{13}C]pyruvate hyperpolarization, conventional magnetic resonance imaging, echocardiography, and blood testing, every 4 weeks for 16 weeks. They were compared with a weight matched, healthy control group. Conductance catheter examination at the end of the study showed impaired right ventricular systolic function along with compromised left ventricular diastolic function. After 16 weeks, we saw a significant decrease in the conversion ratio of pyruvate/bicarbonate in the left ventricle from 0.13 (0.04) in controls to 0.07 (0.02) in animals with pulmonary banding, along with a significant increase in the lactate/bicarbonate ratio to 3.47 (1.57) compared with 1.34 (0.81) in controls. N-terminal prohormone of brain natriuretic peptide was increased by more than 300%, while cardiac index was reduced to 2.8 (0.95) L/min/m^2 compared with 3.9 (0.95) in controls. Echocardiography revealed no changes.

Conclusion Hyperpolarization detected a shift towards anaerobic metabolism in early stages of right ventricular dysfunction, as evident by an increased lactate/bicarbonate ratio. Dysfunction was confirmed with conductance catheter assessment, but could not be detected by echocardiography. Hyperpolarization has a promising future in clinical assessment of heart failure in both acquired and congenital heart disease.

Keywords magnetic resonance imaging • heart failure • congenital heart disease • Metabolism

Introduction

Right ventricular failure is common in patients with congenital heart disease and pulmonary hypertension with occurrence increasing with age.[1] The level of right ventricular function is, moreover, closely correlated with the prognosis of the disease.[2] Assessment of right ventricular function is difficult. This is because all established techniques for the evaluation of cardiac function were originally developed for evaluating left ventricular function. Even though the introduction of magnetic resonance has made assessment of ventricular function easier, the right ventricle still presents a considerable challenge due to its anatomical placement, complex geometry and morphology.[3]

*Corresponding author. Tel: +45 2625 2525; Fax: 7845 3079. E-mail: peter.agger@clin.au.dk

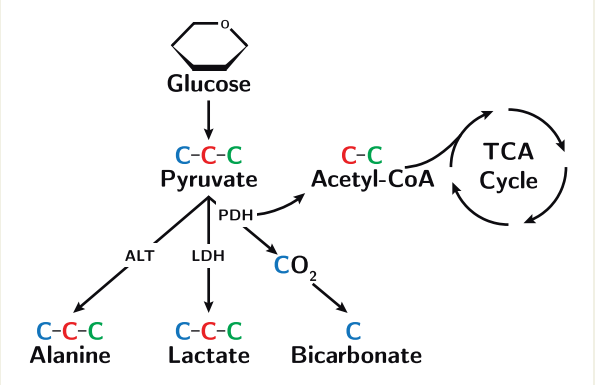

Figure 1 The metabolic pathways of pyruvate. Pyruvate contains three carbon atoms and is formed from glucose through glycolysis. In this study, we hyperpolarize the first carbon atom (blue) making [1-^{13}C]-pyruvate. Using hyperpolarization imaging, we thus follow the metabolic fate of the first carbon atom when pyruvate is metabolized to alanine via alanine transaminase (ALT), lactate via lactate dehydrogenase (LDH), and bicarbonate via pyruvate dehydrogenase (PDH). The second and third carbon atom (red and green) enters the tricarboxylic acid cycle (TCA) when incorporated into acetyl coenzyme A.

Optimal timing for intervention can also be a considerable challenge, which often relies on subjective expert opinions rather than solid clinical data.[4] Reliable diagnostic measures of early right ventricular dysfunction and failure are, therefore, highly sought after.

During development of heart failure, adaptive processes begin at the intracellular level before evolving to a macro-anatomic pathology.[2,5] Intracellular changes could, therefore, provide an early signal of impending right ventricular heart failure. It is hence reasonable to presume that the metabolic alterations during the development of heart failure would appear early in disease progression, and that impaired metabolism is directly linked to the pathogenesis of heart disease.[6]

Pyruvate is rapidly taken up by cardiomyocytes and metabolized through three major pathways (*Figure 1*). It can be converted through anaerobic metabolism to lactate via lactate dehydrogenase, it can be converted to alanine via alanine transaminase[7] or it can be metabolized via pyruvate dehydrogenase to acetyl coenzyme A and CO_2, which is in dynamic equilibrium with bicarbonate via the enzyme carbonic anhydrase.[6] In pressure-overloaded myocardium, increased glycolysis and glucose oxidation is observed. The latter, however, cannot keep pace with the former. This mismatch between glycolysis and pyruvate oxidation is the consequence of increased pyruvate carboxylation and lower flux through pyruvate dehydrogenase, resulting in increased lactate production.[8] The recent introduction of magnetic resonance imaging hyperpolarization has made non-invasive visualization and quantification of metabolic substrates possible.[9] The decreased oxidative capacity in heart failure is detectable with hyperpolarized [1-^{13}C]pyruvate. It is characterized by an increased ^{13}C-lactate signal combined with an almost non-existent ^{13}C-bicarbonate signal. This has been confirmed in dilated cardiomyopathy in pigs,[10] and in hypertrophic cardiomyopathy caused by hyperthyroidism in rats.[11] However, it could not be confirmed in hypertrophy induced by abdominal aortic banding in rats.[12] Hyperpolarization has been suggested as a promising tool for clinical decision-making in adult heart disease.[9] With imminent translation into human studies,[13] this novel technique has the potential to provide important and clinically useful information in the setting of multiple cardiac diseases. Alongside cardiac imaging, biomarkers are increasingly used in diagnosis and monitoring of heart failure. In particular, the N-terminal pro-hormone of brain natriuretic peptide (NT-ProBNP) is commonly used.[14] Fumarase has recently been suggested as a promising biomarker of cell death in both malignant tumours[15] and kidney injury.[16,17] It is a strictly intracellular enzyme that leaks to the blood stream upon cell membrane rupture.[17]

We hypothesized that ^{13}C hyperpolarized magnetic resonance imaging would detect changes in myocardial metabolism as a sign of imminent right ventricular heart failure in pigs. Following 16 weeks of pulmonary artery banding, we expected that decreased bicarbonate levels and increased lactate levels would precede the detection of cardiac ventricular dysfunction by conventional imaging and biochemical measures.

Methods

We have previously shown how our porcine model of right ventricular failure following pulmonary artery banding creates significant right ventricular dysfunction, with a high degree of reproducibility.[18,19] We thus consider this model ideal for the purpose of elucidating the metabolic nature of right ventricular heart failure.

Study design

The study was conducted as a porcine experimental study over a period of 16 weeks.

At baseline 5, Danish Landrace female pigs weighing 8.5 kg were subjected to banding of the pulmonary trunk as outlined in detail in the Supplementary data online and in our previous contributions.[18,19]

The intervention animals were handled every 4 weeks and compared with a weight matched control group at Week 16 ($n = 6$). *Figure 2* outlines the timeline of the experiments and specifies when each of the techniques was used.

At each follow-up point, the animals were assessed with blood samples, 4D echocardiography and conventional and hyperpolarization magnetic resonance imaging. At the end of the study, cardiac performance was assessed using conductance catheter technique.[19] The animals were then euthanized, while still anaesthetized, by exsanguination. All methods are described in detail in the Supplementary data online. The surgical procedures were conducted after approval from the Danish Inspectorate of Animal Experimentation, with the guidelines from this institution complying with 'NIH publication No. 86–23', regarding principles of laboratory animal care (revised 1985).

Statistical considerations

Differences between pulmonary artery banded animals and controls were assessed with a two-tailed Student's *t*-test for normally distributed data and Wilcoxon rank-sum test for non-parametric data. Normal distribution was verified using quantile–quantile plots and histograms. Data from hyperpolarization, magnetic resonance, echocardiography, and biochemistry, were analysed using repeated measurements ANOVA. If statistically significant only baseline and endpoint were compared in the *post hoc* analysis, thus we did not correct for multiple comparisons. Data

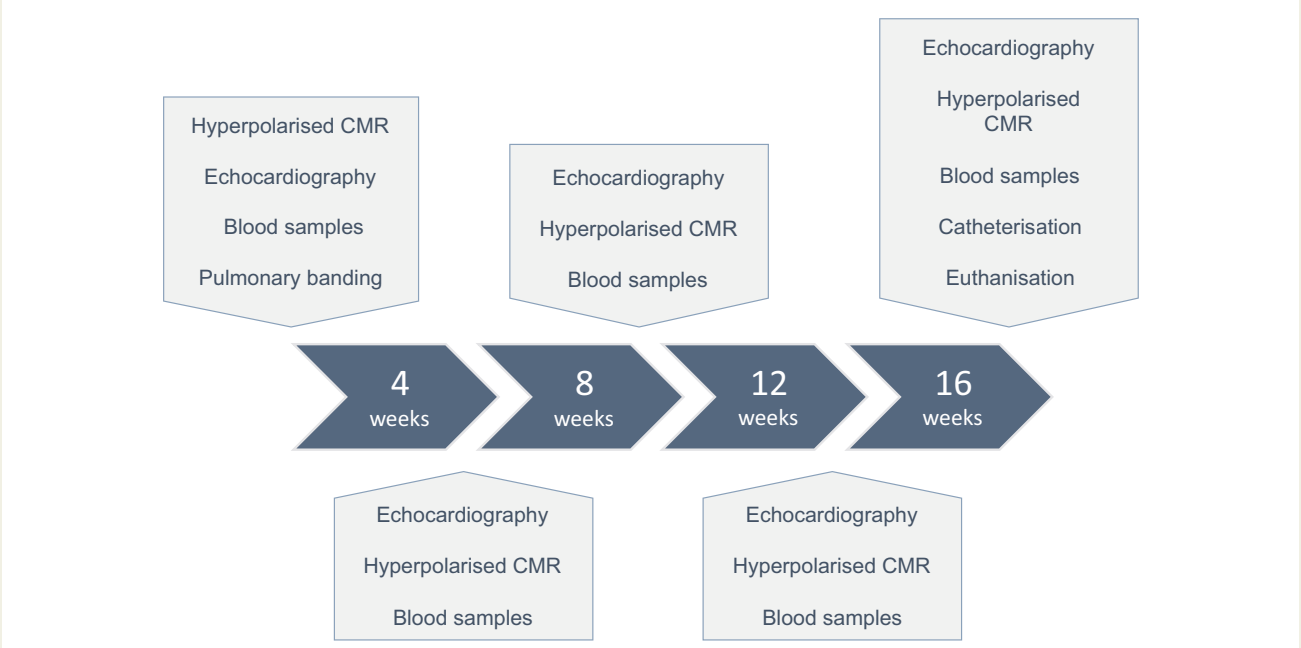

Figure 2 Outline of the study timeline. Animals were subjected to pulmonary banding at Week 0. Every 4 weeks they were subjected to hyperpolarized [1-^{13}C]-pyruvate cardiac magnetic resonance (CMR), 4D echocardiography, and blood samples. Before termination at 16 weeks the animals were, moreover, subjected to biventricular conductance catheter assessment. At all-time points, the events were conducted in the order according to the figure. At Week 16, a weight matched control group was introduced.

are presented as means with standard deviation in parentheses. *P*-values smaller than 0.05 was considered statistically significant.

Results

A total of five animals with a mean weight of 8.5 kg (1.2) underwent banding of the pulmonary trunk. All animals reached Week 16 with no adverse outcomes and no clinical signs of heart failure. At Week 16, banded animals had a mean weight of 37.9 kg (4.5). This was not statistically different from the control group as introduced in Week 16 consisting of six animals with a mean weight of 37.7 kg (0.9), $P > 0.05$. Body surface area was calculated according to the literature.[20] Morphometric data and endpoint characteristics at Week 16 are shown in *Table 1*.

Cardiac hyperpolarization imaging

All data originating from hyperpolarization investigations are shown in *Figure 3*. The ratio of conversion of pyruvate to bicarbonate decreased significantly during the course of the study ($P = 0.02$). At Week 16, the bicarbonate conversion ratio was 0.07 (0.02) in the intervention group vs. 0.13 (0.04) in controls, $P = 0.02$. A significant increase in pyruvate conversion to lactate was found throughout the study. However, no significant difference was found at Week 16 compared with controls. The same applies to the conversion of pyruvate to alanine.

A change in lactate to bicarbonate ratio throughout the study was found to be statistically significant ($P = 0.04$), with an almost linear increase over the first 12 weeks to a ratio of 1.82 (0.92), thereafter increasing abruptly to 3.47 (1.57) in Week 16 compared with 1.34 (0.81) in controls, $P = 0.02$. This shift from bicarbonate to lactate production is illustrated in *Figure 4*. The lactate to alanine ratio at Week 16 was also significantly higher in the intervention group, 1.28 (0.35), as compared with controls 0.86 (0.16), $P = 0.03$. A similar pattern was seen when assessing the alanine to bicarbonate ratio, however, at Week 16 a decrease to 0.41 (0.13) was observed in the banded group, compared with 1.10 (0.58) in controls, $P = 0.03$.

Conventional magnetic resonance imaging

As shown in *Figure 5* and *Table 1* both left and right ventricular end-diastolic volume index were significantly decreased at Week 16 in banded animals, whereas end-systolic volume index was only significantly decreased in the left ventricle. Ejection fraction increased in both ventricles, but was only found to be statistically significant in the left ventricle, where an increase of 25% was found, $P < 0.001$. Changes in wall thicknesses during the course of the study are also shown in *Figure 5*. The left ventricle of the banded animals showed an increase in systolic wall thickness increasing by 30% compared with controls from 9.3 (0.9) to 12.2 (0.2), $P < 0.001$. This increase explains the decreased ventricular volumes and consequently increased left ventricular ejection fraction. Contrary, in the right ventricle differences were found in both systole and diastole. In systole, the right ventricular wall thickness increased from 6.23 (1.2) mm in controls to 8.4 (0.4) in banded animals, an increase of 34%, $P = 0.006$. Likewise, in diastole, it increased from 3.4 (0.6) to 4.9 (1.2), an increase of 41%, $P = 0.03$. The septum-lateral to anterior–posterior ratio indicative of left ventricular deformation was found unaltered during the course of the study and no differences were found between groups. Cardiac index was assessed by magnetic

Table 1 Conductance catheter assessment at 16 weeks

	PB	Control	*P*-value
Morphometric and haemodynamic indices			
Number of animals (*n*)	5	6	
Weight (kg)	37.9 (4.5)	37.7 (0.9)	NS
Body surface area (m^2)	0.80 (0.06)	0.79 (0.01)	NS
Heart rate (bpm)	71 (8.4)	81 (10.5)	NS
Stroke volume (mL/m^2)	50.4 (10.2)	60.7 (5.4)	NS
Cardiac index ($L/min/m^2$)	2.8 (0.5)	3.9 (0.8)	**0.02**
Ventricular volumes			
RV EDV (mL/m^2)	71 (12.6)	91.6 (12.5)	**0.02**
RV ESV (mL/m^2)	41 (12.6)	55 (12.5)	NS
LV EDV (mL/m^2)	48.5 (7.8)	82 (6.9)	**<0.001**
LV ESV (mL/m^2)	20.2 (3.7)	49.5 (6.5)	**<0.001**
RV ejection fraction (%)	56.5 (10.3)	50.9 (9.6)	NS
LV ejection fraction (%)	71.2 (8.4)	56.8 (4.5)	**<0.001**
Systolic indices			
RV PRSW ($mmHg \cdot mL \cdot mL^{-1}$)	15.5 (5.3)	8 (4)	**0.03**
RV dP/dt_{max} (mmHg/s)	543 (53)	399 (87)	**0.01**
RV ESPVR (mmHg · mL)	1.1 (0.6)	0.34 (0.05)	**0.02**
RV P_{max} (mmHg)	43.9 (9.4)	27.3 (1.5)	**<0.001**
RV Ea (mmHg/mL)	1.28 (0.4)	0.6 (0.1)	**<0.001**
RV Ea/ESPVR ratio	1.4 (0.4)	1.9 (0.5)	NS
LV PRSW ($mmHg \cdot mL \cdot mL^{-1}$)	42.8 (10.9)	42.5 (3.6)	NS
LV dP/dt_{max} (mmHg/s)	1411 (316)	1094 (290)	NS
LV ESPVR (mmHg · mL)	1.2 (0.4)	1.0 (0.11)	NS
LV P_{max} (mmHg)	80.4 (6.7)	84.9 (4.5)	NS
LV Ea (mmHg/mL)	2.0 (0.7)	1.7 (0.2)	NS
LV Ea/ESPVR ratio	1.7 (0.5)	1.76 (0.4)	NS
Diastolic indices			
RV tau (ms)	74.2 (18.8)	64.1 (10)	NS
RV EDPVR (mmHg/mL)	0.14 (0.05)	0.16 (0.05)	NS
LV tau (ms)	61.9 (13.7)	46.4 (5.5)	**0.03**
LV EDPVR (mmHg/mL)	0.22 (0.04)	0.17 (0.02)	**0.01**

Data are presented as means (standard deviation). Means compared using Student's *t*-test.
Bold face emphasizes statistical significance.
Ea, arterial elastance; EDV, end-diastolic volume; EDPVR, end-diastolic pressure–volume relation; ESPVR, end-systolic pressure–volume relation; ESV, end-systolic volume; LV, left ventricle; NS, statistically non-significant; P, pressure; PB, pulmonary banding; PRSW, preload recruitable stroke work; RV, right ventricle.

resonance flow measurements. During the first 8 weeks of the study, cardiac index was relatively constant around 5 $L/min/m^2$. Between Week 8 and 12, cardiac index was abruptly reduced to around 2.8 for the remainder of the study, $P = 0.004$. This is shown in *Figure 5*.

Echocardiography

No differences were found when comparing the longitudinal strain, tricuspid annular plane systolic excursion (TAPSE), fractional area change (FAC), *E*/*A* ratios, and *E*′ of banded animals with controls, see *Figure 6*.

Biventricular conductance catheter examination

At Week 16, banded animals had a cardiac index of 2.8 (0.5) $L/min/m^2$ vs. 3.9 (0.8) $L/min/m^2$ in controls, $P = 0.02$. Right ventricular systolic indices such as preload recruitable stroke work, maximum pressure development over time, end-systolic pressure volume relation, maximum pressure, and arterial elastance were all significantly increased, see *Table 1*. No increase was found in left ventricular systolic indices. Conversely, regarding diastolic indices, only the left ventricle was affected. Here, both end-diastolic pressure–volume relation and the isovolumic relaxation constant tau were increased.

Biochemical assessment

An increase in the concentration of NT-ProBNP was found at Week 16, see *Figure 7* and *Table 2*. In pulmonary banded animals a concentration of 19.3 (8.9) pg/mL was found compared with 6.3 (7.0) in controls, $P = 0.02$. Fumarase activity changed significantly through the course of the study ($P = 0.04$), with a peak in Week 8 of 2.2 (0.33). No difference was found when comparing with the control group at Week 16. Also, no significant changes were found in terms of conventional arterial blood gas analyses with acid–base status as shown in *Table 2*. Lastly, the plasma level of pyruvate was decreased at the end of the study from 115.5 (32.5) in the control group to 66.6 (13.4) in banded animals, $P = 0.01$. In spite of this plasma lactate/pyruvate ratio was unchanged. A Pearson's correlation test was performed to assess the relationship between the lactate/pyruvate ratio in the plasma of the two groups, and as with assessment by hyperpolarization, no correlation was found $r = -0.14$, $P = 0.43$.

Discussion

This is the first study to utilize hyperpolarization to assess the metabolic consequences of right ventricular overload in a large animal model. We show that assessment of myocardial metabolism with hyperpolarization is more sensitive in detecting functional changes in early heart failure than conventional right ventricular echocardiography. We suggest the lactate/bicarbonate ratio as a potential new marker of early-stage heart failure. Hyperpolarization showed the lactate/bicarbonate ratio to be increased after 16 weeks, reflecting a shift in the balance of lactate and bicarbonate production, mainly caused by a decreased conversion of pyruvate to bicarbonate. This balance has previously been paralleled with the balance between anaerobic and aerobic metabolism in the ischaemic heart.[21] Our findings are echoed in three recent studies; firstly in pacemaker induced dilated cardiomyopathy in pigs[10] showing decreased pyruvate to bicarbonate conversion along with unchanged conversion to lactate; secondly in a study of hypertrophy induced by hyperthyroidism showing not only decreased conversion to bicarbonate, but also increased conversion to lactate[11]; and lastly in a study if left ventricular pressure overload the conversion to bicarbonate was unchanged, but the lactate levels increased resulting in the same overall increase in lactate/bicarbonate ratio.[12]

Using the conductance catheter technique, we documented significant cardiac dysfunction in the animals with decreased cardiac index, including right ventricular systolic dysfunction and impaired left ventricular diastolic function. Combined with increased NT-proBNP

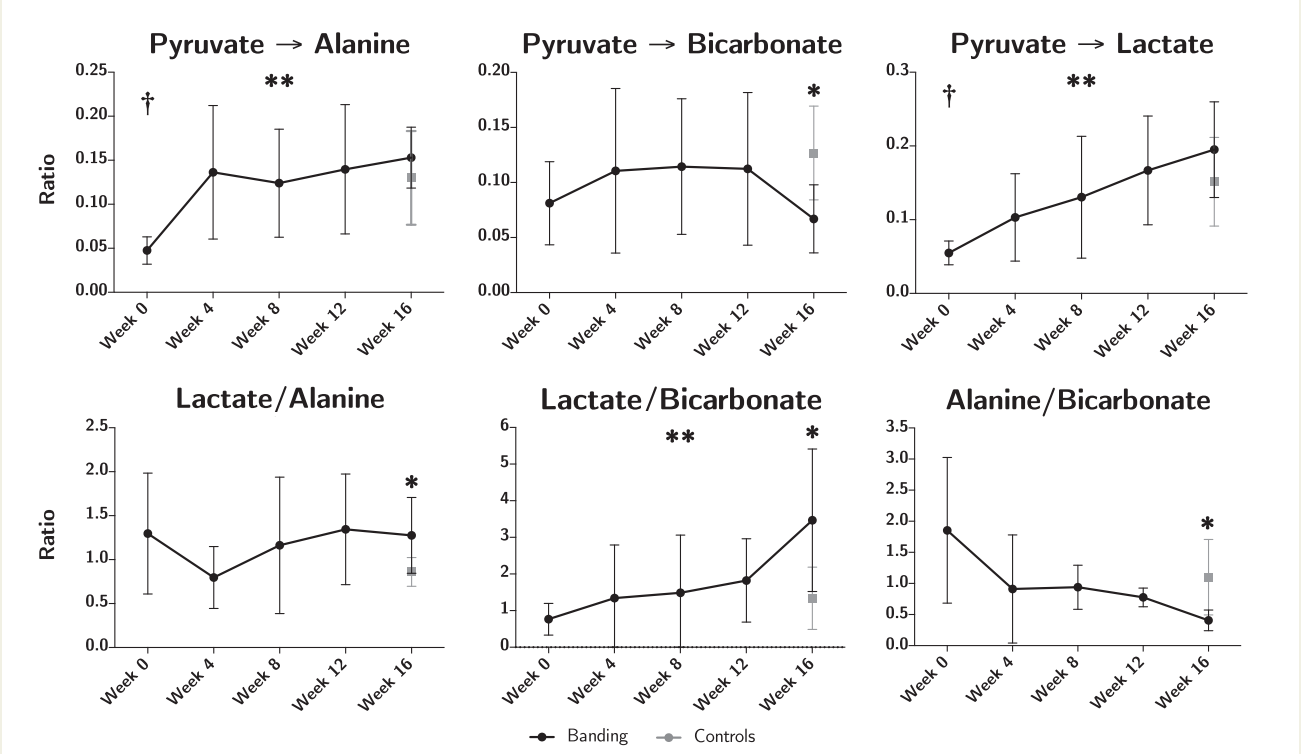

Figure 3 Results on metabolic imaging displayed as pyruvate conversion ratios in the top row and metabolite ratios in the bottom row. Animals subjected to pulmonary banding (black) are compared with the endpoint control group (grey). Data plotted as means with whisker bars representing 95% confidence interval. *Statistically significant difference between the intervention and control group at Week 16. **Statistically significant repeated measures ANOVA in the intervention group. †Statistically significant difference between baseline at Week 0 and the control group.

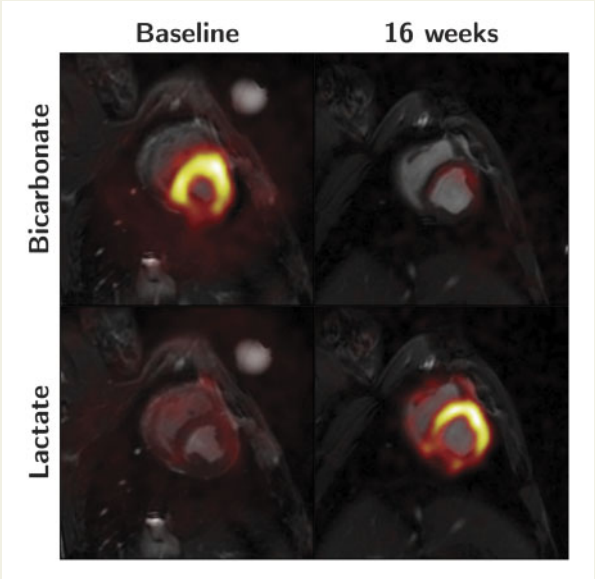

Figure 4 This figure shows the inverse relationship between the conversion of pyruvate to bicarbonate and lactate during the development of right heart failure. ^{13}C signal overlay on conventional short-axis proton images of the heart. Left column is baseline images at Week 0. Right column is at 16 weeks. Top row shows the bicarbonate signal. Bottom row shows the lactate signal.

levels, these findings convey the early onset of heart failure, this pathology was, however, not detectable with conventional measures by echocardiography, see *Figure 6*. Conclusively, it does not seem that metabolic changes precede functional alterations, but the sensitivity of echocardiography at present is not sufficient to detect the disease at this early stage.

As of today heart failure is a clinical diagnosis with many faces.[22] It seems to be commonly accepted that the substrate for the cardiac metabolism change during heart failure.[23] In the healthy heart the main source of ATP is fatty acid oxidation and to a lesser extent glucose oxidation.[23,24] As heart failure progresses towards its end-stage, this balance shifts towards oxidation of pyruvate originating from glycolysis and lactate oxidation.[25] Ultimately, the myocardium is forced to revert to anaerobic glycolysis, leading to lactate increase and decreased oxidative phosphorylation.[10,24,26] Our results indicate that this change towards anaerobic metabolism is initiated early in the development of right heart failure, as we detected an increased lactate/bicarbonate ratio before the clinical signs of heart failure occurred.

Ball *et al.*[21] investigated acute and chronic infarction in a rat model using hyperpolarized pyruvate. They found increased lactate/bicarbonate ratio in the hypoxic area of acute ischaemia. In the present study of right ventricular dysfunction with pathological hypertrophy, a degree of myocardial hypoxia[5] and cell death is anticipated. This would lead to leakage of fumarase into the blood stream.[17] Interestingly, the plasma levels of fumarase were identical between

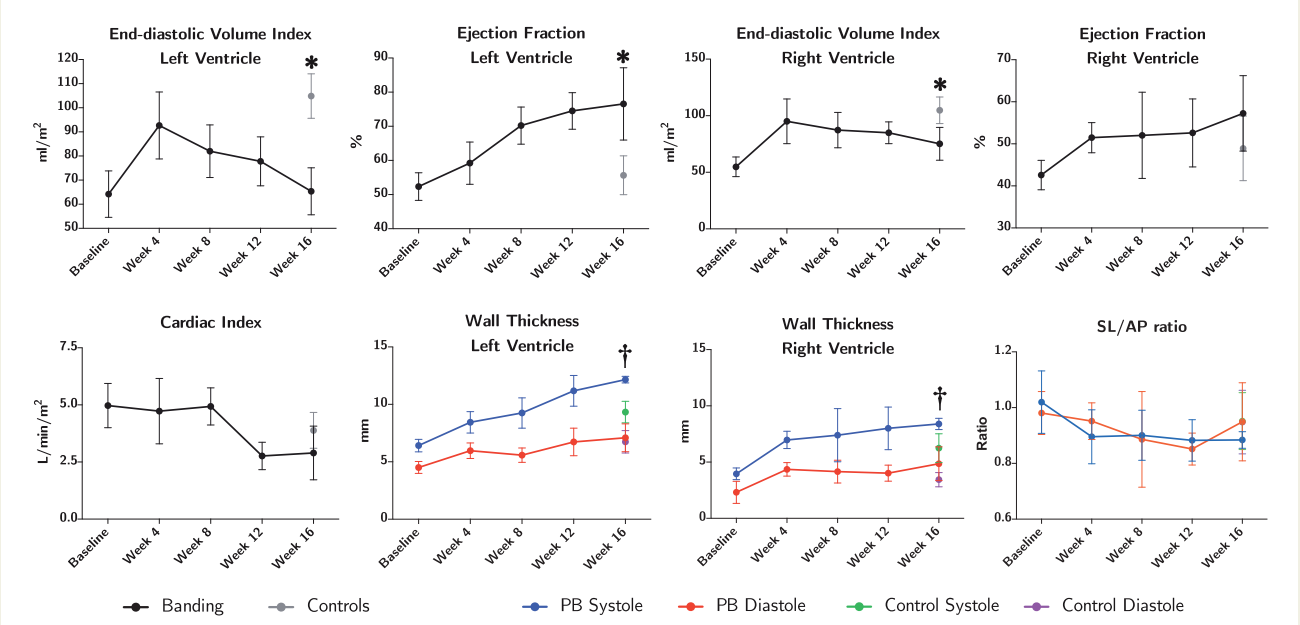

Figure 5 Results of magnetic resonance imaging. Data plotted as means with whisker bars representing 95% confidence interval. PB, pulmonary banding; SL/AP, septum-lateral/anterior-posterior ratio of the left ventricle. *Statistically significant difference between the intervention and control group at Week 16. †Statistically significant one-way ANOVA between groups at 16 weeks.

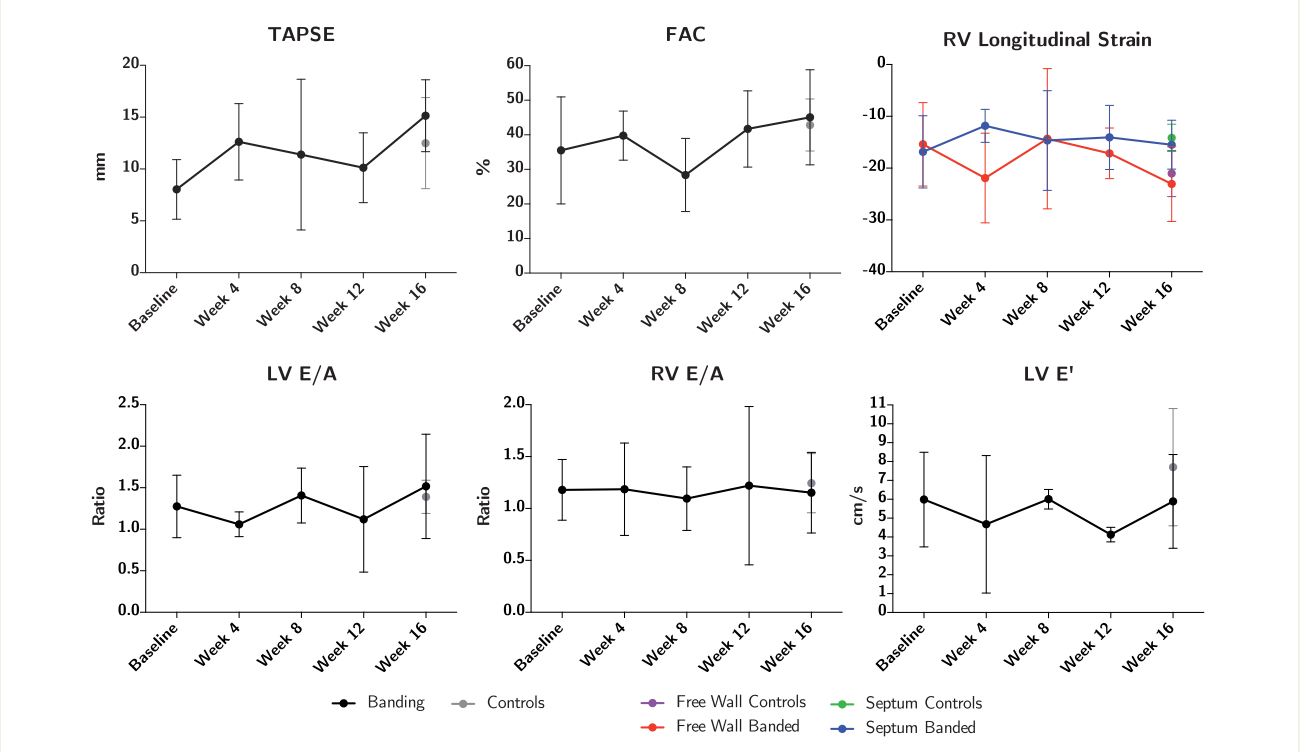

Figure 6 Assessment of cardiac function by echocardiography. Strain is assessed in both the right ventricular free wall, and in the septum. Animals subjected to pulmonary banding (black) are compared with the endpoint control group (grey). Data plotted as means with whisker bars representing 95% confidence interval. FAC, fractional area change; LV, left ventricle; RV, right ventricle; TAPSE, tricuspid annular plane systolic excursion.

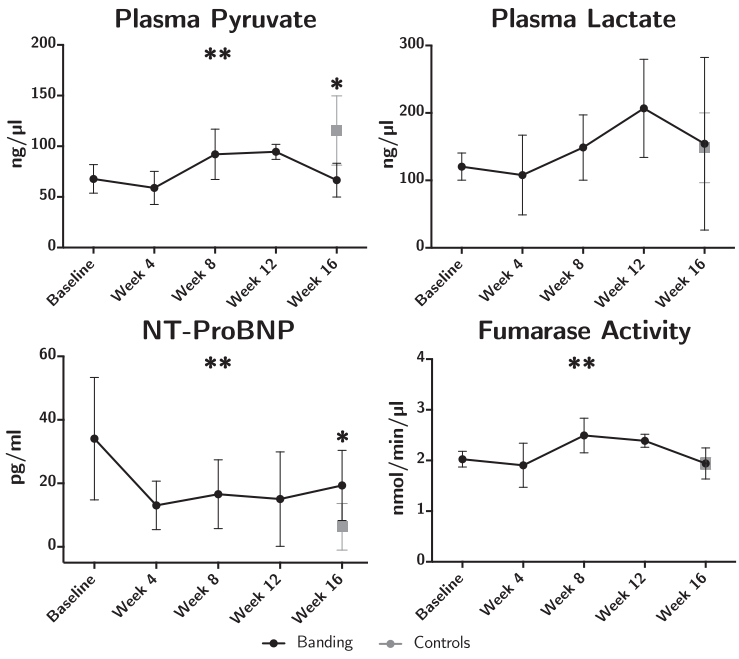

Figure 7 Biochemistry assessment. Animals subjected to pulmonary banding (black) are compared with the endpoint control group (grey). Data plotted as means with whisker bars representing 95% confidence interval. NT-ProBNP, N-terminal pro-hormone of brain natriuretic peptide. *Statistically significant difference between the intervention and control group at Week 16. **Statistically significant repeated measures ANOVA in the intervention group.

Table 2 Biochemical assessment at 16 weeks

Biochemical indices	PB	Control	*P*-value
Arterial blood samples			
pH	7.51 (0.05)	7.52 (0.03)	NS
pCO_2 (kPa)	5.5 (0.8)	5.5 (0.5)	NS
pO_2 (kPa)	28.0 (13.5)	16.4 (3.2)	NS
Sat O_2 (%)	100 (0.6)	99 (1.4)	NS
Base excess (mmol/L)	10.2 (2.0)	10.1 (1.2)	NS
Bicarbonate (mmol/L)	33.2 (1.8)	32.8 (0.7)	NS
Venous blood samples			
Glucose (mmol/L)	3.8 (1.5)	5.1 (0.9)	NS
Lactate (ng/µL)	154.4 (103.1)	148.4 (49.3)	NS
Pyruvate (ng/µL)	66.6 (13.4)	115.5 (32.5)	**0.01**
Fumarase activity (nmol/min/µL)	1.9 (0.25)	1.9 (0.11)	NS
NT-ProBNP (pg/mL)	19.3 (8.9)	6.3 (7.0)	**0.02**

Data are presented as means (standard deviation). Means compared using Student's *t*-test.
Bold face emphasizes statistical significance.
NS, statistically non-significant; NT-ProBNP, N-terminal of the pro-hormone brain natriuretic peptide; PB, pulmonary banding.

the groups, both when comparing Weeks 4 and 8 and when comparing with controls at Week 16. Moreover, the entrance of metabolites into the tricarboxylic acid cycle was largely maintained, or even increased, as evidenced by the reduced alanine/bicarbonate ratio. Alanine can be used as a surrogate for the uptake or intracellular levels of pyruvate.[27] This could indicate that myocardial cell death in the setting of early ventricular dysfunction is largely dominated by apoptosis, and not myocardial necrosis as seen in ischaemia–reperfusion injury.[16] Pyruvate constitutes the intersection of several important metabolic pathways.[28] Contemplating the fate of pyruvate in the myocardium provides insight into myocardial metabolism as a whole (*Figure 1*). It is tempting to conclude that the observed increase in lactate/bicarbonate ratio indicates a shift towards anaerobic metabolism. This is probably an oversimplification. Although not reaching statistical significance, an increased arterial oxygen partial pressure was observed following right ventricular overload. We have, however, neither assessed the oxygen consumption of the tissue nor the oxygen levels within the tissue. Therefore, we cannot explicitly conclude whether the decrease in pyruvate dehydrogenase activity is brought upon by hypoxia, and hence true anaerobic metabolism, or if it is simply a part of the aetiology of heart failure.

We detected a 46% decreased in the conversion of pyruvate to bicarbonate. This finding is echoed in other studies investigating heart failure in dilated cardiomyopathy[10] and hypertrophic cardiomyopathy induced by hyperthyroidism.[11] This suggests that impaired oxidative metabolism is a common pathway in heart failure. The only study to disagree with this concept is by Dodd *et al.*,[29] they report increased bicarbonate production in the hypertrophied myocardium of spontaneously hypertensive rats

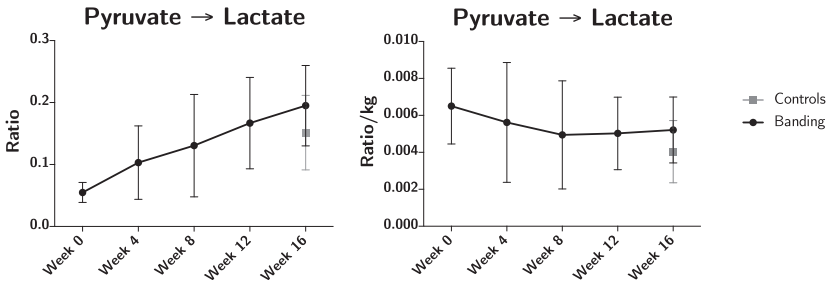

Figure 8 Pyruvate to lactate conversion ratios with (right) and without (left) body weight normalization. The pronounced difference between the curves underscores the age/weight related development in metabolic phenotype.

exhibiting a compensated state of dysfunction without heart failure. The spontaneously hypertensive rat, however, carries a mutation in the fatty acid transporter CD36, which may explain the disagreement with our findings.

Natural metabolic alterations in the myocardium during ageing

It is known that myocardial metabolism changes through life,[24] and most dramatically in the perinatal period.[1] Over the 16 week period we saw a significant decrease from 34 to 13 pg/mL of NT-ProBNP, $P = 0.04$, this was to be expected considering NT-proBNP is significantly higher during early infancy in humans.[30] *Figure 8* shows the conversion rate of pyruvate to lactate presented with and without weight correction. It supports the notion that the metabolic and biochemical changes observed during the first 4 weeks of the study can be attributed to natural development rather than early initiation of heart failure. Natural metabolic changes with age need to be taken into account in future studies of myocardial metabolism in congenital heart disease. Hyperpolarization seems an interesting and useful modality for this purpose.

Study limitations

For ethical reasons we have chosen only to include a control group at the end of the study. This limitation makes it difficult to draw finite inferences on the metabolic changes during ageing. When correcting for body weight as in *Figure 8*, our data suggest that growth indeed influences metabolism, but our data should be interpreted with care in this matter. In the light of this, we must note that intervention animals were handled and anaesthetized five times as opposed to once in the control group. However, we consider 4 weeks sufficient for total recovery from anaesthesia, but the influence of several sedations on hyperpolarization has never been investigated. Lastly, results of hyperpolarization are assessed in the left ventricular myocardium, because the spatial resolution does not allow us to assess the thin-walled right ventricle. Until the technique's spatial resolution is improved, we can only use it as an indirect measure of right ventricular dysfunction. We, therefore, only assessed the left ventricular metabolic consequences of right ventricular pressure overload. Hence we do not know whether the metabolic results can be directly translated to the right ventricle, this constitutes an important limitation of this study. During right-sided heart failure, significant reductions in left ventricular systolic and diastolic function are observed.[19] This can be explained by the transfer of electrical, mechanical and biochemical signals between the ventricles through interventricular cross-talk.[31,32] This is evident from *Figure 4*, showing changes in the left ventricular myocardium to be more pronounced than in the right ventricle, this is in spite of the isolated right ventricular pressure overload. As mentioned, myocardial metabolism is multifaceted and each pathway could potentially be affected in right ventricular pressure overload. Although [1-^{13}C]pyruvate as bioprobe is a relevant choice, our approach may overlook other important and highly relevant metabolic events that may explain or contribute to heart failure. In the future other probes could be used to look into other heart failure mechanisms or perhaps target even earlier events in the progression of the disease.

Conclusion

The present study is the first to investigate right ventricular dysfunction in a human compatible large animal model using hyperpolarization. We conclude that hyperpolarization is capable of detecting a shift towards anaerobic metabolism before conventional echocardiography can detect impaired right ventricular function. A complete magnetic resonance assessment of structure, function and metabolism provides the most complete evaluation of the progression of heart failure in the setting of right ventricular pressure overload. It must, therefore, be considered a multi-modality task to monitor the development of heart failure.[33] In this regard, hyperpolarization has a very promising future in the diagnosis and monitoring of heart failure in both adult and congenital heart disease.

Supplementary data

Supplementary data are available at *European Heart Journal - Cardiovascular Imaging* online.

Acknowledgements

The authors are grateful to Dr Marie A. Schroeder for scientific comments on the manuscript and to Dr Robert S. Stephenson for linguistic editing and scientific comments.

Funding

The study was generously supported by the Danish Children Heart Foundation (16-R99-A5074-26040 and 15-R98-A5048-26028).

Conflict of interest: none declared.

References

1. Hinton RB, Ware SM. Heart failure in pediatric patients with congenital heart disease. *Circ Res* 2017;**120**:978–94.
2. Voelkel NF, Quaife RA, Leinwand LA, Barst RJ, Mcgoon MD, Meldrum DR *et al.* Right ventricular function and failure report of a national heart, lung, and blood institute working group on cellular and molecular mechanisms of right heart failure. *Circulation* 2006;**114**:1883–91.
3. Friedberg MK, Redington AN. Right versus left ventricular failure: differences, similarities, and interactions. *Circulation* 2014;**129**:1033–44.
4. Stout KK, Broberg CS, Book WM, Cecchin F, Chen JM, Dimopoulos K *et al.* Chronic heart failure in congenital heart disease: a scientific statement from the American Heart Association. *Circulation* 2016;**133**:770–801.
5. Bogaard HJ, Abe K, Noordegraaf AV, Voelkel NF. The right ventricle under pressure: cellular and molecular mechanisms of right-heart failure in pulmonary hypertension. *Chest* 2009;**135**:794–804.
6. Doenst T, Nguyen TD, Abel ED. Cardiac metabolism in heart failure: implications beyond ATP production. *Circ Res* 2013;**113**:709–24.
7. Taegtmeyer H, Peterson MB, Ragavan VV, Ferguson AG, Lesch M. *De novo* alanine synthesis in isolated oxygen-deprived rabbit myocardium. *J Biol Chem* 1977;**252**:5010–8.
8. Lahey R, Carley AN, Wang X, Glass CE, Accola KD, Silvestry S *et al.* Enhanced redox state and efficiency of glucose oxidation with miR based suppression of maladaptive NADPH-dependent malic enzyme 1 expression in hypertrophied hearts. *Circ Res* 2018;**122**:836–45.
9. Malloy CR, Merritt ME, Sherry AD. Could 13C MRI assist clinical decision-making for patients with heart disease? *NMR Biomed* 2011;**24**:973–9.
10. Schroeder MA, Lau AZ, Chen AP, Gu Y, Nagendran J, Barry J *et al.* Hyperpolarized (13)C magnetic resonance reveals early- and late-onset changes to *in vivo* pyruvate metabolism in the failing heart. *Eur J Heart Fail* 2013;**15**:130–40.
11. Atherton HJ, Dodd MS, Heather LC, Schroeder MA, Griffin JL, Radda GK *et al.* Role of pyruvate dehydrogenase inhibition in the development of hypertrophy in the hyperthyroid rat heart: a combined magnetic resonance imaging and hyperpolarized magnetic resonance spectroscopy study. *Circulation* 2011;**123**:2552–61.
12. Seymour AM, Giles L, Ball V, Miller JJ, Clarke K, Carr CA *et al. In vivo* assessment of cardiac metabolism and function in the abdominal aortic banding model of compensated cardiac hypertrophy. *Cardiovasc Res* 2015;**106**:249–60.
13. Cunningham CH, Lau JY, Chen AP, Geraghty BJ, Perks WJ, Roifman I *et al.* Hyperpolarized 13C metabolic MRI of the human heart: initial experience. *Circ Res* 2016;**119**:1177–82.
14. Sato Y, Fujiwara H, Takatsu Y. Biochemical markers in heart failure. *J Cardiol* 2012;**59**:1–7.
15. Gallagher FA, Kettunen MI, Brindle KM. Biomedical applications of hyperpolarized 13C magnetic resonance imaging. *Prog Nucl Magn Reson Spectrosc* 2009;**55**:285–95.
16. Miller JJ, Lau AZ, Nielsen PM, Mcmullen-Klein G, Lewis AJ, Jespersen NR *et al.* Hyperpolarized [1,4-$^{13}C_2$]fumarate enables magnetic resonance-based imaging of myocardial necrosis. *JACC Cardiovasc Imaging* 2017;**11**:1594–606.
17. Nielsen PM, Eldirdiri A, Bertelsen LB, Jørgensen HS, Ardenkjaer-Larsen JH, Laustsen C. Fumarase activity: an *in vivo* and *in vitro* biomarker for acute kidney injury. *Sci Rep* 2017;**7**:40812.
18. Nielsen EA, Smerup M, Agger P, Frandsen J, Ringgard S, Pedersen M *et al.* Normal right ventricular three-dimensional architecture, as assessed with diffusion tensor magnetic resonance imaging, is preserved during experimentally induced right ventricular hypertrophy. *Anat Rec* 2009;**292**:640–51.
19. Hyldebrandt JA, Sivén EE, Agger P, Frederiksen CA, Heiberg J, Wemmelund KB *et al.* Effects of milrinone and epinephrine or dopamine on biventricular function and hemodynamics in an animal model with right ventricular failure after pulmonary artery banding. *Am J Physiol Heart Circ Physiol* 2015;**309**:H206–12.
20. Kelley KW, Curtis SE, Marzan GT, Karara HM, Anderson CR. Body surface area of female swine. *J Anim Sci* 1973;**36**:927–30.
21. Ball DR, Cruickshank R, Carr CA, Stuckey DJ, Lee P, Clarke K *et al.* Metabolic imaging of acute and chronic infarction in the perfused rat heart using hyperpolarised [1-13C]pyruvate. *NMR Biomed* 2013;**26**:1441–50.
22. Maciver DH, Dayer MJ. An alternative approach to understanding the pathophysiological mechanisms of chronic heart failure. *Int J Cardiol* 2012;**154**:102–10.
23. Neubauer S. The failing heart—an engine out of fuel. *N Engl J Med* 2007;**356**:1140–51.
24. Stanley WC, Recchia FA, Lopaschuk GD. Myocardial substrate metabolism in the normal and failing heart. *Physiol Rev* 2005;**85**:1093–129.
25. Recchia FA, Mcconnell PI, Bernstein RD, Vogel TR, Xu X, Hintze TH. Reduced nitric oxide production and altered myocardial metabolism during the decompensation of pacing-induced heart failure in the conscious dog. *Circ Res* 1998;**83**:969–79.
26. Evans RD, Clarke K. Myocardial substrate metabolism in heart disease. *Front Biosci (Schol Ed)* 2011;**4**:556–80.
27. Lewandowski ED. Metabolic heterogeneity of carbon substrate utilization in mammalian heart: NMR determinations of mitochondrial versus cytosolic compartmentation. *Biochemistry* 1992;**31**:8916–23.
28. Rider OJ, Tyler DJ. Clinical implications of cardiac hyperpolarized magnetic resonance imaging. *J Cardiovasc Magn Reson* 2013;**15**:93.
29. Dodd MS, Ball DR, Schroeder MA, Le Page LM, Atherton HJ, Heather LC *et al. In vivo* alterations in cardiac metabolism and function in the spontaneously hypertensive rat heart. *Cardiovasc Res* 2012;**95**:69–76.
30. Schwachtgen L, Herrmann M, Georg T, Schwarz P, Marx N, Lindinger A. Reference values of NT-proBNP serum concentrations in the umbilical cord blood and in healthy neonates and children. *Z Kardiol* 2005;**94**:399–404.
31. Smerup M, Nielsen E, Agger P, Frandsen J, Vestergaard-Poulsen P, Andersen J *et al.* The three-dimensional arrangement of the myocytes aggregated together within the mammalian ventricular myocardium. *Anat Rec (Hoboken)* 2009;**292**:1–11.
32. Agger P, Lakshminrusimha S, Laustsen C, Gugino S, Frandsen JR, Smerup M *et al.* The myocardial architecture changes in persistent pulmonary hypertension of the newborn in an ovine animal model. *Pediatr Res* 2016;**79**:565–74.
33. Surkova E, Muraru D, Iliceto S, Badano LP. The use of multimodality cardiovascular imaging to assess right ventricular size and function. *Int J Cardiol* 2016;**214**:54–69.